

## A Procedure for Application of the Three-Omega Method to Measurement of Gas Thermal Conductivity\*

Elin YUSIBANI<sup>\*\*</sup>, Peter Lloyd WOODFIELD<sup>\*\*\*</sup>, Shogo MOROE<sup>\*\*</sup>,  
Kanei SHINZATO<sup>\*\*\*</sup>, Masamichi KOHNO<sup>\*\*</sup>, Yasuyuki TAKATA<sup>\*\*</sup>  
and Motoo FUJII<sup>\*\*\*</sup>

<sup>\*\*</sup> Department of Mechanical Engineering, Kyushu University, 744 Motooka Nishi-ku Fukuoka, Japan

<sup>\*\*\*</sup> Research Center for Hydrogenius, AIST, 744 Motooka Nishi-ku Fukuoka, Japan

E-mail: e-yusibani@aist.go.jp

### Abstract

A non-linear least-squares curve-fitting procedure is proposed to analyze three-omega voltage data from a fine wire in a gas sample using the three-omega method. The method uses both three-omega components of the voltage arising from a sinusoidal heating current to determine the thermal conductivity of the surrounding medium. The proposed procedure is tested against simulated data and some experimental data for air at atmospheric pressure. Treating the technique as an absolute method and assuming a known sample heat capacity, the thermal conductivity of air has been measured at room temperature to within 11% of a reference value. Practical application of the method may require a calibrated effective wire length and wire diameter. An average wire temperature rise of around 10 K to ensure the three-omega components is enough for accurate measurement.

**Key words:** Air, Thermal Conductivity, Curve Fitting, Three-Omega, Heat Capacity

### 1. Introduction

A Literature survey has revealed that hydrogen gas thermal conductivity experimental data at high temperature and high pressure are scarce [1]. Moreover, studies related to application of the three-omega method to measurement of gas-phase properties are limited [2,3,4]. Reference-quality gas thermal conductivity data is usually measured by the transient-hot-wire method [5]. This is a very powerful and accurate technique. However, it has a disadvantage that it usually requires two long wires and a thus fairly large sample. The three-omega method appears to be an attractive alternative to the transient hot-wire method since the small penetration depth suggests that even in a very small pressure vessel it may be possible to avoid the influence of the boundary condition at the wall of the vessel. However, assumptions made in the three-omega theory need confirmation in order to establish the validity of the method for gas property measurement [2,3]. Our future interest is to measure hydrogen gas thermal conductivity at high pressure and high temperature with this method. Therefore, it may be desirable to have a small sample in a small pressure vessel. For high-pressure hydrogen, a small pressure vessel is required for safety and ease of conformity with high-pressure gas regulations. The transient short-hot-wire method [6] overcomes the difficulty of the sample size but for low-density gases the temperature rise of the wire is still strongly influenced by

the boundary condition at the cell wall [7]. The three-omega method has been used successfully for measurements of the thermal conductivity of solid materials [8]. Also, by increasing the frequency, the effect of the cell wall boundary condition can be avoided. However, there are a number of difficulties to be overcome and as mentioned above, few studies have been done on application of the three-omega method to the thermal conductivity of gases.

Recently we found by simulation that measurement of gas-phase thermal conductivity by the three-omega method is likely to be difficult because a non-linear curve is produced when the in-phase three-omega component is plotted against the logarithm of frequency [2]. We also found that end effects are important at low frequency for low thermal conductivity samples [3]. An example of these effects is shown in Fig. 1 where the three-omega voltage components are simulated for air at ambient temperature. The hot wire dimensions for the simulation are chosen to be 10  $\mu\text{m}$  and 15.6 mm in diameter and length, respectively. The circular symbols (straight lines) are from a simulation of the three-omega voltage components where we have omitted the wire heat capacity. The dashed lines (non-linear curves) include the wire heat capacity in the calculation. Finally, the solid lines include the end effect correction in the calculation (again non-linear lines). The non-linear result for gas is in contrast to results for water [9] and solids [8] where we can simply obtain the thermal conductivity by direct measurement of the gradient of the in-phase three-omega voltage.

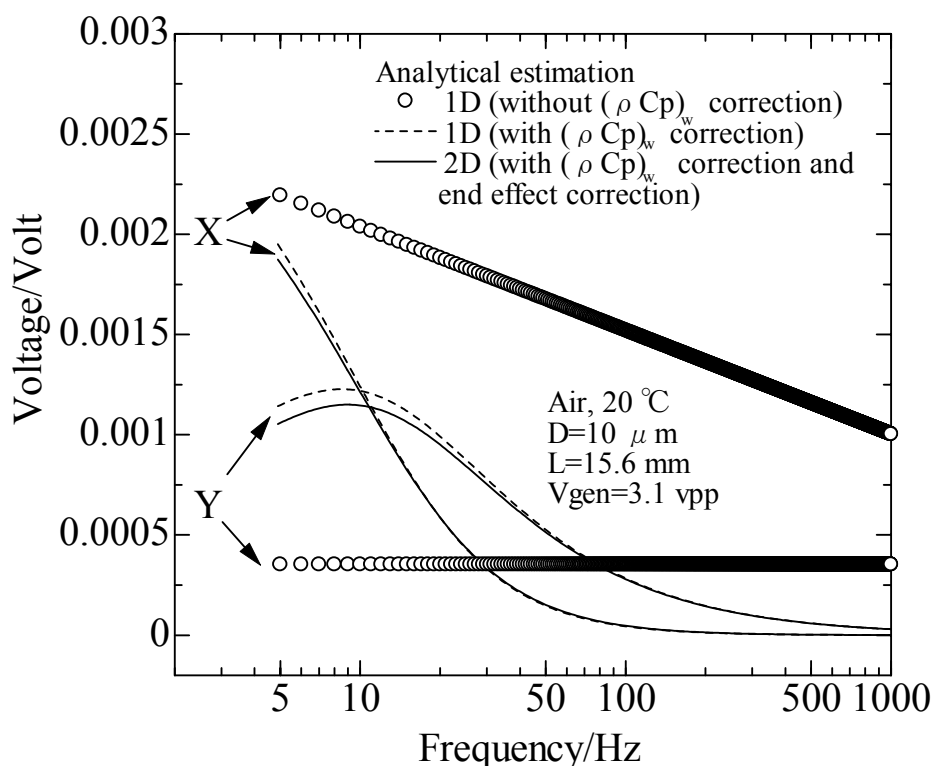


Fig. 1 The three-omega voltage components simulation for Air at 20 °C, 0.1013 MPa. Solid lines include wire heat capacity ( $(\rho c_p)_w$ ) and end effect correction

It is clear from Fig. 1 that the wire heat capacity is largely responsible for the non-linearity in the three-omega voltage component versus frequency curve and end effects are important in the low-frequency range. Unfortunately, taking the wire heat capacity and end effect correction into account in the calculation produces a somewhat tedious equation that does not permit explicit evaluation of thermal conductivity and thermal diffusivity. In our previous

study [2] we concluded that either the wire should be very fine (nano-scale) to avoid the effects of the wire heat capacity, or a curve-fitting procedure would be necessary to analyze the data. In the present study, we propose a suitable non-linear least-squares curve-fitting method to derive thermal conductivity from the experimental data for a gas sample. The procedure is tested against analytical computer-generated-data and experimental data for air at atmospheric pressure. The method is flexible in that it can be adapted easily to consider different combinations of independent variables, although the main goal is to determine the thermal conductivity ( $\lambda$ ). Firstly, we consider using  $\lambda$  as the only unknown assuming that we have a reasonable estimate of the volumetric heat capacity of the gas. We also consider analyzing the experimental data for air using both  $\lambda$  and the diffusivity,  $\alpha$  as unknown independent variables to be measured.

## 2. Governing equation

### 2.1 Two-dimensional analytical solution including wire heat capacity and end effects

Recently we derived a two-dimensional analytical solution to the problem of a heated wire of finite length and finite heat capacity with isothermal boundaries assumed at the ends of the wire [3]. We will describe the solution and assumptions briefly here. The full derivation can be found in Ref. [3]. Neglecting natural convection and radiation, unsteady two-dimensional heat conduction in the sample ( $r > r_o$ ) is governed by the differential equation of conduction of heat in an isotropic solid.

$$\frac{1}{r} \frac{\partial T}{\partial r} + \frac{\partial^2 T}{\partial r^2} + \frac{\partial^2 T}{\partial z^2} = \frac{1}{\alpha_s} \left( \frac{\partial T}{\partial t} \right) \quad (1)$$

The boundary condition at the wire/sample interface ( $r = r_o$ ) is defined by including the axial temperature gradient in the wire and wire heat capacity. The radial temperature gradient in the wire is neglected.

$$-2\pi r_o \lambda_s \frac{\partial T}{\partial r} \Big|_{r=r_o} = \frac{P}{l} + \pi r_o^2 \lambda_w \frac{\partial^2 T}{\partial z^2} \Big|_{r=r_o} - \pi r_o^2 (\rho c_p)_w \frac{\partial T}{\partial t} \Big|_{r=r_o} \quad (2b)$$

Assuming frequency is high enough so that the effect of the cell wall can be neglected. The boundary conditions in the far field and at the cold end and center of the wire are given by

$$T \Big|_{r \rightarrow \infty} = 0 \quad ; \quad T \Big|_{z=0} = \frac{\partial T}{\partial z} \Big|_{z=l/2} = 0 \quad (2c)$$

Using an oscillating electric current,  $I = I_o \cos(\omega t)$ , the power is given as  $P = I_o^2 R \cos^2(\omega t)$ . Rather than using an initial condition, we assume that time is large enough so that only steady oscillating terms remain in the solution. Also the transient effect of the direct-current component of the power is neglected. The current source input at a frequency  $\omega$  induces temperature oscillations at the doubled frequency  $2\omega$ . By making use of the assumption  $|(2\omega/\alpha)^{1/2} r_o j^{1/2}| \ll 1$ , finally we obtain the temperature oscillation,  $T_{2\omega}$ , at the doubled frequency,  $2\omega$ , in the frequency domain. To determine the voltage, the resistance of the hot wire is given as a linear function of the hot wire temperature. This temperature oscillation results in a voltage oscillation across the heating element that includes tripled frequency components at  $3\omega$ . Thus the three-omega voltage components can be expressed by the form [3]

$$V_{3\omega} = X \cos(3\omega) + Y \sin(3\omega) \quad (3)$$

where  $X$  and  $Y$  are given as

$$X = \frac{I_o^3 R_{0C} R_T \beta}{\pi^3} \sum_{n=1}^{\infty} \frac{1}{m_n^2} \left( \frac{BD - AC}{C^2 + D^2} \right) \quad (4)$$

$$Y = \frac{I_o^3 R_{0C} R_T \beta}{\pi^3} \sum_{n=1}^{\infty} \frac{1}{m_n^2} \left( \frac{AD + BC}{C^2 + D^2} \right)$$

$$A = \ln \left( \frac{r_o}{2} \left( \frac{4\omega^2}{\alpha_s^2} + m_n^4 \right)^{1/4} \right) + \gamma \quad ; \quad B = \frac{1}{2} \tan^{-1} \left( \frac{2\omega}{\alpha_s m_n^2} \right) \quad (4a)$$

$$C = \lambda_s - A \frac{r_o^2 \lambda_w m_n^2}{2} + B r_o^2 (\rho_c)_w \omega \quad ; \quad D = r_o^2 (\rho_c)_w \omega A + B \frac{r_o^2 \lambda_w m_n^2}{2} \quad (4b)$$

$$m_n = \frac{2n-1}{l} \pi \quad (4c)$$

Equation (4) is the basis for obtaining thermal conductivity and (if possible) thermal diffusivity simultaneously via a curve-fitting method. It also can be used to find suitable instrument settings and an appropriate frequency range for measuring the three-omega voltage components before starting the experiment.

### 2.2 Phase-Angle Analysis

It is apparent from Eq. (4) that the coefficient,  $I_o^3 R_{0C} R_T \beta / (\pi^3)$  is the same for both the in-phase ( $X$ ) and out-of-phase ( $Y$ ) components of the  $3\omega$  voltage. Therefore the phase angle between the triple of the  $1\omega$  current and the  $3\omega$  voltage is independent of the magnitude of  $I_o$ ,  $R$  and  $\beta$ . For this reason we are also interested in considering the ratio  $X/Y$  which is the cotangent of the phase angle,  $\phi$ .

$$\cot \phi = \frac{1}{\tan \phi} = \frac{X}{Y} \quad (5)$$

Substituting Eq. (4) into Eq. (5), we would like to propose and test an alternative base equation for determining the sample thermal conductivity by the  $3\omega$  method as follows

$$\frac{X}{Y} = \frac{\sum_{n=1}^{\infty} \frac{1}{m_n^2} \left( \frac{BD - AC}{C^2 + D^2} \right)}{\sum_{n=1}^{\infty} \frac{1}{m_n^2} \left( \frac{AD + BC}{C^2 + D^2} \right)} \quad (6)$$

Thus in the present study we consider using either Eq. (4) or Eq. (6) as the base equation for connecting the experimental data and the theoretical model.

## 3. Curve-Fitting Method

### 3.1 Curve-Fitting Algorithm

The object of the curve-fitting method is to find  $\lambda$  such that the analytical equation agrees with the measured three-omega voltage components ( $X$  and  $Y$ ). Since we are also testing the possibility of determining both  $\lambda$  and  $\alpha$  simultaneously, we will outline the more general case here. This can be described as a non-linear least-squares problem (Eq. (7)), where we need to find  $\lambda$  and  $\alpha$  such that  $S_{\text{non-linear}}$  is minimized. To solve a somewhat similar non-linear problem, Woodfield et al. [7] recently proposed a curve-fitting procedure to find  $\lambda$  and  $\alpha$  in the transient short-hot-wire method. We follow a similar approach here except that the voltage from Eq. (4) is used in the function to be minimized rather than the wire temperature from a numerical simulation. The algorithm used to achieve this is shown in Fig. 2. The method starts with guessing the initial values of  $\lambda$  and  $\alpha$  which are then iteratively adjusted so that the analytical solution finally agrees with the experimental data. The unknown parameters are perturbed one at a time by a small amount ( $\delta\lambda$  and  $\delta\alpha$ ) and then the three-omega voltages are recalculated at

each experimental point. Assuming that the effect of the perturbation on the change in  $X$  and  $Y$  is linear, the linear least-squares problem given in Eq. (8) can be solved in order to obtain new estimates of the unknown parameters. For the present study,  $\delta\lambda$  and  $\delta\alpha$  are taken to be 1% of the current estimated value for  $\lambda$  and  $\alpha$ , respectively. This approach has an advantage over the more commonly used Newton's method for non-linear problems in that it is not necessary to differentiate Eq. (4) analytically with respect to the unknown parameters  $\lambda$  and  $\alpha$ .

$$S_{\text{non-linear}} = \sum_{i=1}^{N_{\text{exp}}} (X_{\text{exp } i} - X_i(\lambda, \alpha))^2 + (Y_{\text{exp } i} - Y_i(\lambda, \alpha))^2 = \min \quad (7)$$

$$S_{\text{linear}} = \sum_{i=1}^{N_{\text{exp}}} ((X_{\text{exp } i} - X_i) - x_{\alpha}(X_i' - X_i) - x_{\lambda}(X_i'' - X_i))^2 + \sum_{i=1}^{N_{\text{exp}}} ((Y_{\text{exp } i} - Y_i) - x_{\alpha}(Y_i' - Y_i) - x_{\lambda}(Y_i'' - Y_i))^2 = \min \quad (8)$$

Equation (8) is solved with the linear least-squares method using Gram-Schmidt ortho-normalization and Q-R factorization. By choosing initial guesses for  $\lambda$  and  $\alpha$  within  $\pm 50\%$  of the actual values, the above algorithm is found to converge by about 6 iterations. The method simplifies a little when using  $\lambda$  as the only unknown variable assuming we have a reasonable approximation for the volumetric heat capacity  $\rho c_p$  of the sample. In addition, we tested the same procedure with the cotangent of the phase angle ( $X/Y$ ) as given by Eq. (6) instead of using Eq. (4).

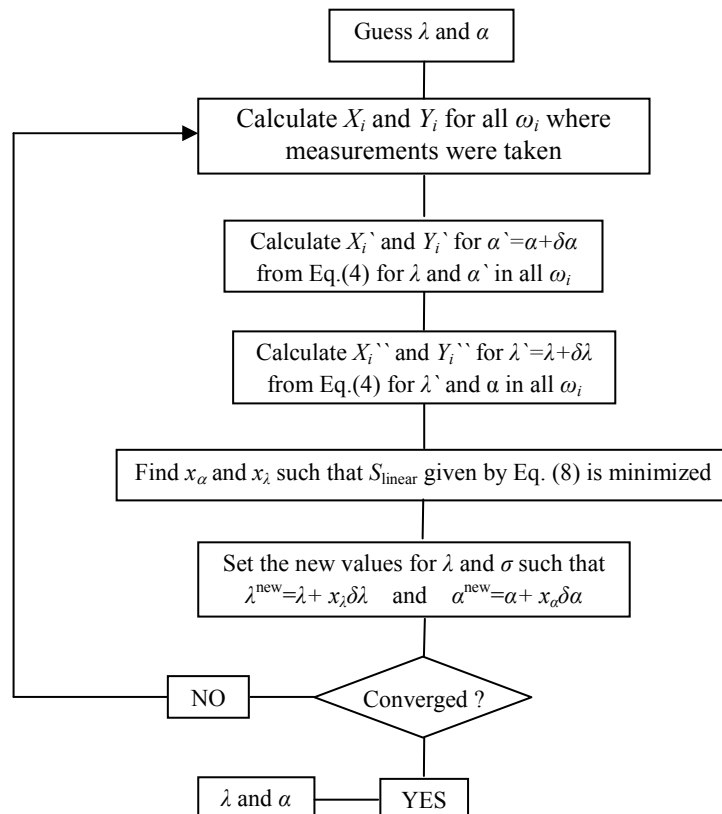


Fig. 2 The curve-fitting algorithm to determine  $\lambda$  and  $\alpha$

### 3.2 Testing of the Algorithm with Computer-Generated Data

Before considering the experimental data, it is important to demonstrate the self-consistency and the convergence of the curve-fitting procedure. We tested the algorithm with the computer-generated data for 20, 100 and 1000 data points using gas sample properties corresponding to air at 24 °C and atmospheric pressure. The test data was generated using the analytical solution shown in Eqs. (4). Then starting from arbitrary initial guesses the algorithm shown in Fig. 2 was applied to test if it would return the correct values for  $\lambda$  and  $\alpha$ . We truncated the generated data to five significant figures as an optimistic approximation to the

possible accuracy of the acquired three-omega voltage data set. The deviations from the exact simulation values are tabulated on the Table 1.

Table 1 Analysis of computer-generated data compared with exact simulation values

No. of data	Deviation from exact simulation value	
	$\lambda$ (%)	$\alpha$ (%)
20	0.004	-0.04
100	0.002	-0.03
1000	0.0008	0.002

At five significant figures, we can reach 0.004% accuracy for thermal conductivity and 0.04% for thermal diffusivity assuming that there is no error in the model itself. The simulated result did not change much by using more than 20 data points. An example of the convergence of the curve-fitting algorithm is shown in Table 2. Starting at initial guesses with errors of the order of 10%, the algorithm converges by about four iterations for this example.

Table 2 Search algorithm convergence for 100 data points (variables:  $\lambda$  and  $\alpha$ )

Step	Thermal Conductivity ( $\text{Wm}^{-1}\text{K}^{-1}$ )	Thermal Cond. error (%)	Thermal Diffusivity ( $10^{-5} \text{m}^2\text{s}^{-1}$ )	Thermal Diff. error (%)
Initial guess	0.03	14.626	2.0000	-8.62
1 <sup>th</sup> Iteration	0.024248701	-7.349	1.35657	-38.03
2 <sup>th</sup> Iteration	0.026071525	-0.384	2.34682	7.21
3 <sup>th</sup> Iteration	0.026165856	-0.023	2.18901	0.0004
4 <sup>th</sup> Iteration	0.026171501	-0.002	2.18852	-0.03
5 <sup>th</sup> Iteration	0.026171362	-0.002	2.18844	-0.03
6 <sup>th</sup> Iteration	0.026171365	-0.002	2.18845	-0.03

Reference:  $\lambda=0.02617 \text{ Wm}^{-1}\text{K}^{-1}$ ;  $\alpha= 2.189 \times 10^{-5} \text{ m}^2\text{s}^{-1}$

#### 4. Experiment

Lock-in-amps are the most common choice for the measurement of the three-omega voltage components in the three-omega method. However, some researchers have suggested the use of analog/digital converters and Fourier transforms to analyze the data [10]. In the present study, experiments were done with a lock-in-amp and repeated with a high-speed analog/digital converter for comparison.

##### 4.1 Experimental Set Up

The AC sinusoidal signal is generated from a signal generator, model WF1974 (NF Corporation). The three-omega voltage component from the probe is extracted by a lock-in-amp DSP model 7265, manufactured by Signal Recovery and the signal was also analyzed using an A/D board (model PXI5922) manufactured by National Instruments. The circuit is shown in Fig. 3a. The Pt-wire-sensor cell is arranged in series with a reference resistor. The value of resistance reference was chosen to be almost similar to the probe resistance so that the voltage input range on both channels of the A/D board is similar. The reference resistor has a resistance of 25  $\Omega$  and the Pt-wire resistance was measured to be 21.407  $\Omega$  at a temperature of 20°C. The time constant for the lock-in-amp was set equal to 1 s.

The details of the Pt-wire-sensor cell are shown in Fig. 3b. The diameter and length of the Pt-wire-sensor are 10  $\mu\text{m}$  and 15.6 mm, respectively. The material for the 1.5 mm diameter supporting leads is also platinum to avoid Seebeck effects at the connections to the 10  $\mu\text{m}$  wire. The fine platinum wire is spot welded to the platinum leads. The internal volume of the cell is about 33  $\text{cm}^3$  and experiments are performed at different voltages and at various

frequencies. In the present study we report data at frequencies up to 1000 Hz where the function generator voltage setting was 2.0 Vp-p and 3.1 Vp-p. These voltages correspond to an oscillating current magnitude of  $I_0 \approx 10$  mA and 16 mA, respectively. The general properties of the present experimental set up are shown in Table 3. A thermostatic bath was used and the sample temperature was assumed to be the same as the set temperature of 20°C. The temperature coefficient of resistance,  $\beta$ , was determined by measuring the resistance at different temperatures from 20 to 60°C with the platinum wire immersed in a liquid toluene sample. The Pt-wire-sensor radius was taken to be the nominal value of 5  $\mu\text{m}$ . Scanning electron microscope (SEM) measurements of the diameter of a sample of the wire from the same roll suggested a departure of less than 0.1  $\mu\text{m}$  from the nominal value. The length of the Pt-wire-sensor was measured to be around 15.6 mm. However, it was difficult to determine the length more accurately than  $\pm 0.5$  mm due to uncertainty in the locations of the weld positions.

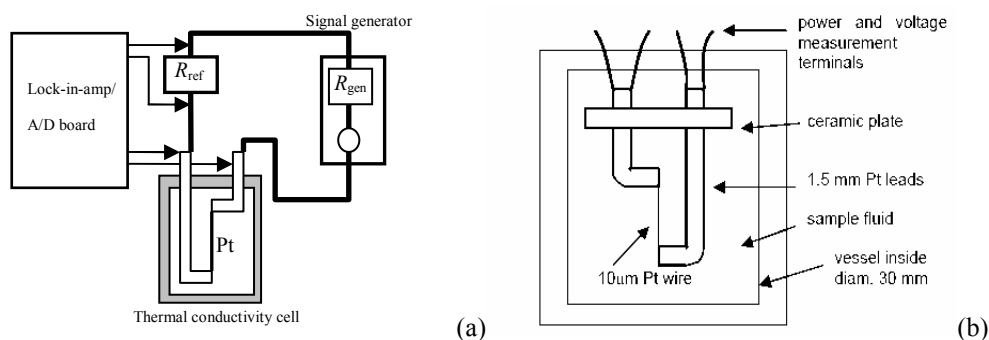


Fig. 3 (a) Schematic diagram of measurement system for three-omega method (b) the design of the thermal conductivity cell

Table 3 Parameters for Experiment

Parameter	Value	Parameter	Value
Bath Temperature / °C	20.00	Pt-sensor radius ( $r_0$ ) / $\mu\text{m}$	$5.0 \pm 0.1$
Pressure / MPa	0.101	Pt-sensor length ( $l$ ) / mm	$15.6 \pm 0.5$
Resistance at 0 °C ( $R_{0C}$ ) / $\Omega$	19.877	$\lambda(\text{REFPROP}) / \text{Wm}^{-1}\text{K}^{-1}$	0.0258
Resistance ref. ( $R_{\text{ref}}$ ) / $\Omega$	25	$\alpha(\text{REFPROP}) / \text{m}^2\text{s}^{-1}$	$2.189 \times 10^{-5}$
TCR ( $\beta$ ) / $\text{K}^{-1}$	0.00385	$(\rho c_p)_w / \text{Jm}^{-3}\text{K}^{-1}$	$2.820 \times 10^6$

#### 4.2 A/D Board Data Analysis

Since measuring  $3\omega$  components with an A/D converter is not as common as using a lock-in-amp, it is important to outline some details of the procedure used to analyze the data from the A/D converter. The raw data from the A/D converter are measured voltages across the hot wire and reference resistor as a function of time. In principle, any data set with time period greater than one full oscillation of the  $1\omega$  component can be analyzed to find the Fourier components in the frequency domain. For the present study, a period of 0.8 s was used. Since the resistance of the reference resistor does not change with time, the current flowing through the circuit is in phase with voltage across the reference resistor (assuming its inductance is negligible). On the other hand, the voltage across the probe is slightly out of phase with respect to the voltage across the reference resistor due to the transient heating of the wire. This phase difference plays a role in distinguishing between in-phase ( $X$ ) and out-of-phase ( $Y$ ) three-omega components. Therefore, firstly we need to anchor the analysis starting time,  $t_0$ , for a cosine signal in the voltage across the reference resistor. For an example, Fig. 4 shows raw voltage data across the reference resistor.

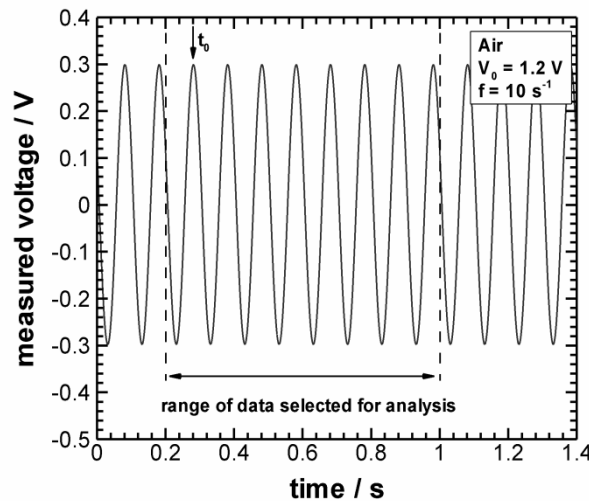


Fig.4 Sample of raw data for voltage across the reference resistor

The dotted lines show the beginning and end of the data set selected for analysis. The time axis in Fig. 4 corresponds to the time from when the A/D board started sampling. The starting time,  $t_0$ , for a cosine signal with no sine component corresponds to the first maximum after the first dotted line. This can be found accurately without user intervention by determining  $A$  and  $B$  in Eq. (9) using the least-squares method.

$$V_{\text{ref}} \approx A \cos(\omega t) + B \sin(\omega t) = \sqrt{A^2 + B^2} \cos(\omega(t - t_0)) \quad ; \quad t_0 = \frac{\tan^{-1}(B/A)}{\omega} \quad (9)$$

For the present analysis,  $\omega$  is assumed to be the same as the setting on the function generator,  $\omega = 2\pi f$ . Once  $t_0$  and  $\omega$  are decided then the probe voltage data can be analyzed by assuming:

$$\begin{aligned} V_p = & V_{\text{offset}} + A_1 \cos(\omega(t - t_0)) + B_1 \sin(\omega(t - t_0)) + \\ & A_2 \cos(2\omega(t - t_0)) + B_2 \sin(2\omega(t - t_0)) + \\ & X \cos(3\omega(t - t_0)) + Y \sin(3\omega(t - t_0)) + \\ & A_4 \cos(4\omega(t - t_0)) + B_4 \sin(4\omega(t - t_0)) + \dots \end{aligned} \quad (10)$$

The coefficients of the three-omega components  $X$  and  $Y$  are the values to be determined. For the present analysis, it is assumed that Fourier series was truncated at the  $6\omega$  components. The least-squares method was then used to determine the coefficients in Eq. (10) including  $X$  and  $Y$ .

#### 4.3 Correction for $3\omega$ components in the current

Equation (4) above was derived assuming that the current contains no  $3\omega$  components and is simply given by  $I = I_0 \cos(\omega t)$ . However, for the circuit used in the experiment (Fig. 3) unwanted  $3\omega$  currents will certainly be present. One source of such currents is imperfections in the generated signal. However, the main source is due to the fact that the function generator in Fig. 3a produces an oscillating voltage rather than a pure oscillating current. Because of this, the  $3\omega$  voltage component across the hot wire will in turn produce an additional  $3\omega$  component in the current. By neglecting higher-order terms, to correct for this difference between the model and the experiment, the  $3\omega$  components given in Eq. (4) need to be multiplied by the factor  $(R_{\text{gen}} + R_{\text{ref}})/(R_p + R_{\text{gen}} + R_{\text{ref}})$  (assuming a perfect signal generator  $V_{\text{gen}3\omega} = 0$ ). Derivation of this correction factor is given in Ref. [2]. This approach makes the electrical circuit simpler than that of Cahill [8] but has the disadvantage that  $3\omega$  components of the current flowing through the circuit from causes other than the oscillating voltage signal generator are not automatically subtracted. Also, unlike Cahill's method, it is necessary to know the internal resistance of the function generator,  $R_{\text{gen}}$  in the present analysis. Fortunately, in the case of the two-channel A/D converter we can measure the  $3\omega$  current flowing through the reference resistor directly by performing a Fourier analysis of the voltage across the reference resistor. Therefore for the A/D board experiment we can also directly subtract the  $3\omega$

voltage components due to the unwanted  $3\omega$  components in the current. This provides an additional check for use of the above-mentioned correction factor  $(R_{\text{gen}}+R_{\text{ref}})/(R_{\text{p}}+R_{\text{gen}}+R_{\text{ref}})$  and an indication of how much of the  $3\omega$  current is due to other sources. For the case of the lock-in-amp, such a direct subtraction cannot be done without extra instrumentation in the circuit (e.g. see Ref. [8]).

## 5. Results

### 5.1 Data Analyzed using both In-Phase and Out-of-Phase Components (Eq. 4)

Figure 5a shows the magnitude of the three-omega voltages measured with the lock-in-amp and best-fit curves using the present analysis method with the function generator set at 3.1 Vpp ( $I_0 \approx 16$  mA). The rectangular-white symbols are the in-phase components (X) and rectangular-black symbols are the out-of-phase components (Y). The dashed and solid lines are results from the analytical estimation (Eq. (4)) and the present curve-fitting analysis using the thermal conductivity as the unknown variable. For this case the present method gave a deviation of about 4 % from the reference value. When we applied  $\lambda$  and  $\alpha$  as the unknown variables, we found that for the particular case shown in Fig. 5a, the deviation of  $\alpha$  from the reference value [11] was more than 100%. Generally, the thermal diffusivity value gives a much bigger deviation from the reference value in comparison with the thermal conductivity result. We suppose that the heat capacity of the gas has to change by a reasonably large amount in order to have a significant influence on the measured three-omega voltage components. Therefore we can conclude that the present method using Eq. (4) may not be suitable for simultaneously determining both thermal conductivity and thermal diffusivity.

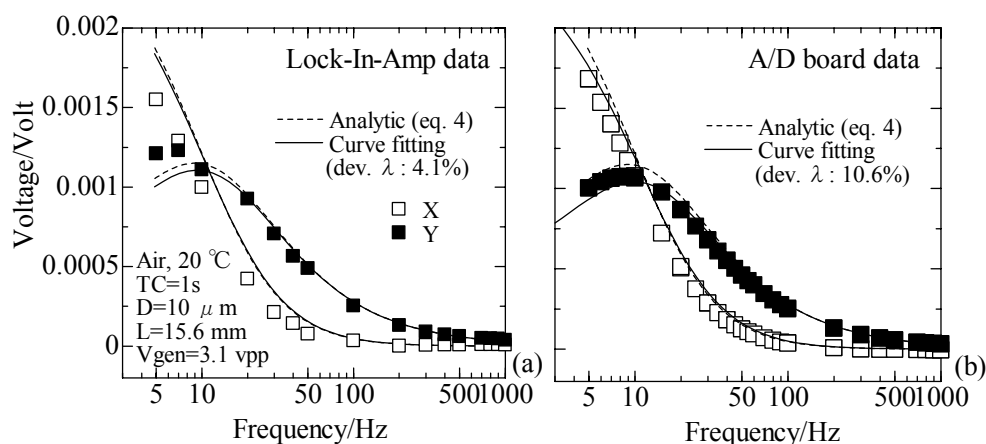


Fig. 5 Curve-fitting line versus experimental data for air at 20 °C with function generator voltage 3.1Vp-p ( $I_0 \approx 16$  mA) obtained by (a) lock-in-amp (b) A/D board

Figure 5b shows experimental data for the same conditions as in Fig. 5a but obtained with Fourier analysis of the A/D board data. For this case we found that the measured thermal conductivity is almost 11 % higher than the reference value. This deviation is larger than that obtained from the lock-in-amp. Compared with the lock-in-amp, the A/D board has more flexibility but requires additional effort to analyze the data. Surprisingly, the three-omega components measured in the present study by the A/D board in Fig. 5b appear to have less scatter than those from the lock-in-amp (Fig. 5a). Thus we can confirm that the high-speed A/D converter is a possible alternative instrument for use in the three-omega method. In both Figs. 5a and 5b the best-fit result from curve fitting is not as good as was hoped. This suggests a systematic difference between the model and the experiment. It was found that a much better fit to the experimental data could be obtained if the diameter and the length of the wire were replaced with an effective diameter and effective length from calibration.

5.2 Data Analyzed using the Cotangent of the Phase Angle (Eq. 6)

According to Eq. (6) the phase angle between the triple of the  $1\omega$  current and  $3\omega$  voltage is independent of the magnitude of the current. To confirm this we have done an experiment at different voltages, i.e. 2.0 Vpp and 3.1 Vpp. Figure 7a shows the result for the cotangent of the phase angle (X on Y) without correction for the  $3\omega$  current. The symbols represent measurements while the lines show the curve fitting results. Generally the lock-in-amp data are lower than the data for the A/D board. Surprisingly, the curve fitting values for thermal conductivity measured by the A/D board are in better agreement with the reference value than those measured by the lock-in-amp. Also it can be seen that for greater than about 100 Hz the data becomes very scattered. This may be attributed to the noise-to-signal ratio which becomes large at high frequencies where the  $3\omega$  voltages are very small.

Figure 7b shows the A/D board data after correction for the measured  $3\omega$  current in the circuit. At high frequencies the scatter is much smaller than that shown in Fig. 7a. Thus it is clear that  $3\omega$  currents (and/or spurious  $3\omega$  voltages in the measuring system) are the main cause of the scatter in the high-frequency range of the data in Fig. 7a. The correction is effective in the high-frequency range but hardly changes the results for the low-frequency range. Correcting for  $3\omega$  currents also improved the measured value for the thermal conductivity with respect to the reference value. In the case of a signal generator voltage of 2.0 Vpp the thermal conductivity determined from the A/D board data in Fig. 7a was 14% lower than the reference value. However, after correction for  $3\omega$  currents, the measured thermal conductivity improved to 6% lower than the reference value. Thus it is important to eliminate the effects of  $3\omega$  currents in the circuit if Eq. (6) is used for analyzing the data. The good agreement between the two different voltages shown in Fig. 7b also confirms that the phase angle between the  $1\omega$  current and  $3\omega$  voltage is independent of the signal generator voltage.

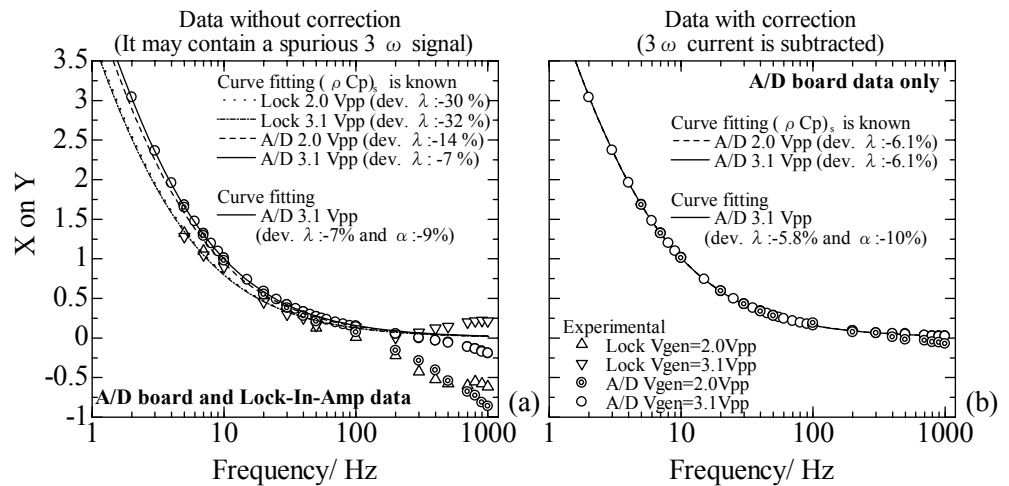


Fig. 7 Curve-fitting line versus experimental data with function generator voltage 2.0 Vpp ( $I_0 \approx 10$  mA) and 3.1Vpp ( $I_0 \approx 16$  mA) obtained by (a)Lock-in-amp and A/D Board without correction term (b) A/D Board only, with correction term

5.3 Temperature Rise and Function Generator Voltages

In order to reduce natural convection effects and to avoid ambiguity in specifying at what temperature the thermal conductivity is measured, it is desirable to keep the current as small as possible. Fig. 8 shows a one-dimensional numerical simulation of the transient wire temperature rise for two different function generator voltages starting at an initially uniform temperature. The case with  $V_{gen} = 1.55 \cos(\omega t)$  corresponds to the function generator settings for 3.1Vpp. For this case the average wire temperature rise was about 9 K by about 3 s after

heating started. Based on Fig. 8 the temperature oscillation for 10 Hz is much larger than that for 500 Hz. It is clear that the maximum temperature rise will correspond to the lowest frequency setting for a given current.

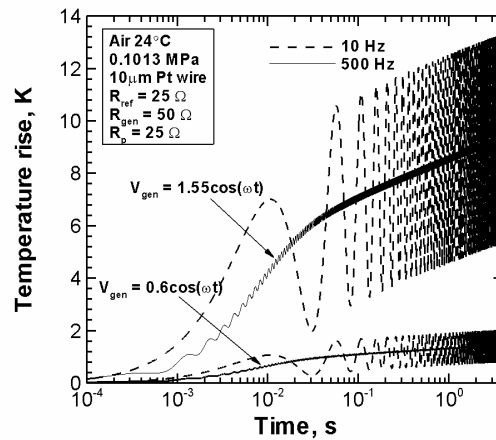


Fig. 8 Wire temperature rise versus time for function generator voltages 3.1Vpp and 1.2Vpp.

Having the function generator voltage so that  $V_{gen} = 0.6 \cos(\omega t)$  (i.e. 1.2 Vpp) leads to a temperature rise that is about 15% of that of the higher voltage as can be seen in Fig. 8. Thus we may conclude that it would be desirable to use a current smaller from the point of view of reducing the temperature rise. Generally we found that if the maximum  $X$  or  $Y$  voltage component is much less than about 1 mV we could not get a good result with the present experimental arrangement. However, if we can improve the present circuit and reduce the noise in the measurement, then a small voltage (i.e. 1.2 Vpp) is recommended in order to reduce possible natural convection effects and decrease the influence of the temperature dependency of the properties. For example, in the application to hydrogen thermal conductivity measurement, a temperature rise of 10 K at atmospheric pressure corresponds to a 2.5 % change in thermal conductivity. However, for pressures as high as 100 MPa, it causes about 1% change in thermal conductivity [11].

#### 5.4 Effect of using a calibrated length and diameter for the wire

We also investigated the possibility of using an effective length and diameter for the Pt-wire-sensor determined from calibration with the reference gas, argon, at 20 °C.

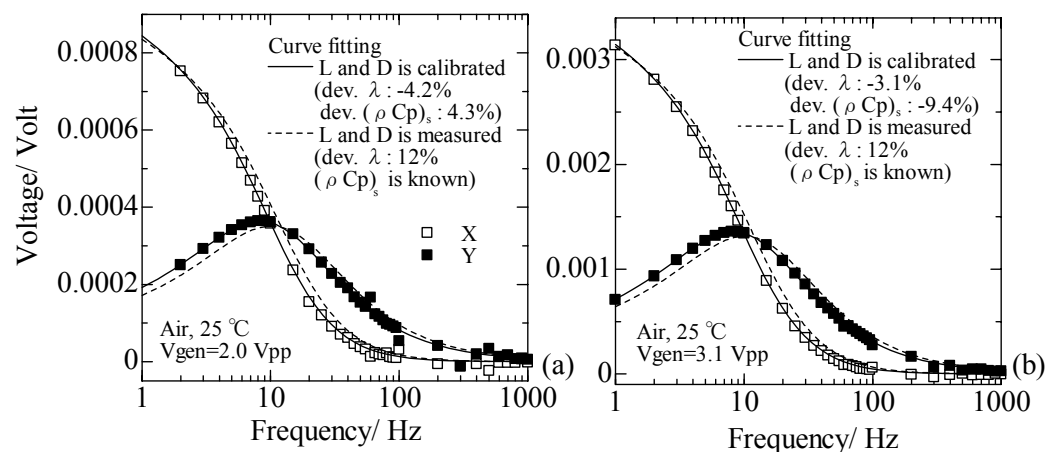


Fig.9 Curve-fitting line versus experimental data with length and diameter calibrated obtained by A/D board at (a) 2.0 Vpp and (b) 3.1 Vpp in voltage

The experiment was conducted at 2.0 Vpp and 3.1 Vpp for the function generator voltage. The geometry of the Pt-wire-sensor was 10.0  $\mu\text{m}$  in diameter (nominal value) and 15.77 mm in length (measured).

We should mention that this Pt-wire-sensor used in this test is slightly longer than that shown in Table 3. After calibration with argon, the effective diameter and length were found to be 10.2  $\mu\text{m}$  and 17.86 mm, respectively. The diameter and the length are increased about 2% and 13%, respectively. Figure 6 shows the curve fitting with and without calibration. The curve fitting shows that the calibration gives a better fit to the experimental data and a better measurement of the thermal conductivity. Based on the Fig.6, we recommend using a calibrated effective wire length and wire diameter for the practical application of the present method.

### 5.5 Summary and Discussion

The measured thermal conductivity using Eq. (4) was higher than the reference value. On the other hand, using Eq. (6) tended to produce an under-estimate of the thermal conductivity. An overestimate for thermal conductivity could suggest a systematic error related to additional heat losses in the cell such as the presence of natural convection. Wang et al. [9] suggested that natural convection effects on the three-omega voltages in fluid measurements decrease with an increase in the frequency. Shulga et al. [12] measured toluene up to 1000 MPa by the oscillating current method. He mentioned that in his experiments, the product  $GrPr$  was always below 1000 due to small deviations of the mean temperature of the wire from the environmental temperature. Moreover, he mentioned that the actual measurements involve only a thin motionless layer of fluid in which no convection can exist. This reasoning explains why high frequencies are preferred for reducing natural convection effects. Recently, S. M. Lee [4], measured dielectric liquids and gases with the three-omega method and found that the measurement is higher than the theory at low frequency. He observed that the result is sensitive to heating power and suspected natural convection is the cause of the error. It may be difficult to avoid natural convection with the three-omega method unless analysis is done within a very short time after switching on the oscillating current and/or by using a small current. This issue needs further experimental and theoretical studies for confirmation.

Issues related to uncertainty in the wire diameter and length, and the accuracy of the voltage measurement may also contribute to the inaccuracy of thermal conductivity measurement in the present study. Some of these issues can be overcome by determining an effective length and diameter for the wire in a fluid/gas of known properties. This approach has also been used successfully in the transient short-hot-wire method [6].

### 6. Conclusions

We can conclude as follows:

- A curve-fitting procedure for finding gas thermal conductivity from measured three-omega voltage components was proposed.
- The method shows promise for measurement of thermal conductivity but it may be difficult to determine the gas heat capacity (thermal diffusivity) simultaneously.
- Practical application of the method to thermal conductivity measurement may require a calibrated effective wire length and radius.
- Issues related to uncertainty in the voltage measurement and natural convection may be the cause for the inaccuracy of the present thermal conductivity measurement. These need to be investigated in future studies.

### Acknowledgement

This research has been conducted as a part of the "Fundamental Research Project on Advanced Hydrogen Science" funded by New Energy and Industrial Technology Development

Organization (NEDO).

### Nomenclature

$(\rho c_p)_w$	volumetric heat capacity of the wire at constant pressure
$(\rho c_p)_s$	volumetric heat capacity of the sample at constant pressure
$I_o$	magnitude of the oscillating current
$l$	half length of the wire-sensor ( $l=L/2$ )
$L$	length of the wire-sensor
$P$	Power
$r_o$	radius of the wire-sensor
$r; z$	r-axis and z-axis
$R_T$	resistance of the wire-sensor at temperature $T$
$R_{0C}$	resistance of the wire-sensor at $0^\circ\text{C}$
$t$	time
$T$	temperature
$V_{3\omega}$	$3\omega$ voltage component
$V_{\text{gen}3\omega}$	$3\omega$ component of the signal generator voltage
$V_{\text{gen}}$	signal generator voltage
$X$	magnitude of $3\omega$ voltage of in-phase component
$Y$	magnitude of $3\omega$ voltage of out-of-phase component
$\alpha_s$	thermal diffusivity of the sample
$\beta$	temperature coefficient of resistance (TCR)
$\gamma$	Euler's constant (0.5772...)
$\lambda_s$	thermal conductivity of the sample
$\lambda_w$	thermal conductivity of the wire-sensor
$\phi$	phase angle
$\omega$	phase frequency ( $=2\pi f$ )

### References

- [1] J. W. Leachman, R. T. Jacobsen, S. G. Penoncello, M. L. Huber, *Int. J. Thermophys.* Vol. 28 (2007), pp. 773
- [2] E. Yusibani, P. L. Woodfield, X. Zhang, K. Shinzato, Y. Takata, M. Fujii, *Int. J. Thermophys.* Vol. 30 No. 2(2009), pp. 397
- [3] E. Yusibani, P. L. Woodfield, M. Kohno, K. Shinzato, Y. Takata, M. Fujii, 2009, *Int. J. Thermophys.* DOI 10.1007/s10765-009-0572-8
- [4] S. M. Lee, *Rev. Sci. Instrum.* Vol 80 (2009), pp. 024901
- [5] J. J. Healy, J. J. de Groot, J. Kestin, *Physica* Vol. 82C (1976), pp. 392
- [6] M. Fujii, X. Zhang, N. Imaishi, S. Fujiwara, T. Sakamoto, *Int. J. Thermophys.* Vol. 18 (1997), pp. 327
- [7] P. L. Woodfield, J. Fukai, M. Fujii, Y. Takata, K. Shinzato, *Int. J. Thermophys.* Vol. 29 (2008), pp. 1299
- [8] D. G. Cahill, *Rev. Sci. Instrum.* Vol. 61 (1990), pp. 802
- [9] Z. L. Wang, D. W. Tang, S. Liu, X. H. Zheng, A. Araki, *Int. J. Thermophys.* Vol. 28 (2007), pp. 1255
- [10] A. Griesinger, W. Heidemann, E. Hahne, *Int. Comm. Heat Mass Transfer* Vol.26 (1999), pp.451
- [11] NIST Chemistry WebBook (<http://webbook.nist.gov/chemistry/>)
- [12] V. M. Shulga, F. G. Eldarov, Yu. A. Atanov and A. A. Kuyumchev, *Int. J. Thermophys.* Vol. 7 No. 6 (1986), pp. 1147